Statistical Modeling of Type Ia SN Flame

James Hugglestone, Tomasz Plewa (Scientific Computing)

Introduction

Our universe is full of explosive events that shape its evolution, and Type Ia supernovae (SNe Ia) are among the most spectacular of them all. These titanic explosions, which can outshine entire galaxies, are the consequence of the terminal evolution resulting in an explosion of a white dwarf star. But how does a compact, dead star become a cosmic bomb of such magnitude? Researchers believe that part of the answer lies in the conductive flames that form inside the white dwarf, which initiate a runaway nuclear reaction that tears the star apart from the inside out.

To understand the process of a SN Ia explosion, we must first look at the pre-main sequence star that gives rise to it. These stars are born from vast clouds of gas and dust that collapse under their own gravity, producing a central region that is hot enough to trigger nuclear fusion in the course of their evolution. As the star burns through its fuel, it eventually exhausts its hydrogen and helium, leaving behind a core of carbon and oxygen (see Chapter 13 in Carroll & Ostlie 2014).

If the star is more massive than about 10 solar masses, it will continue to burn through its elements until it produces a core of iron. But since iron cannot be fused into heavier elements, the star's nuclear reactions come to a halt, and the core collapses under its own weight. This collapse is so violent that it triggers a shockwave that rips through the star's outer layers, causing a massive explosion that we call a core-collapse supernova.

However, for a less massive star, things play out a little differently. In this case, a white dwarf is the remnant of the low-mass star that has exhausted all of its fuel and the remaining material contracted to a small, incredibly dense object. If a white dwarf has a companion star, it can start to accrete material from its partner, gradually increasing its mass.

Eventually, the white dwarf may reach a critical mass known as the Chandrasekhar limit, at which point the temperature and density reach values sufficient to trigger intense localized nuclear burning. This burst of energy is known as ignition and produces a conductive flame, which in turn initiates a runaway thermonuclear reaction that tears the star apart from the inside out. The result is a Type Ia supernova, a cosmic cataclysm that can outshine an entire galaxy for about a month.

In this poster, we will demonstrate how the physics behind SN Ia conductive flames can be represented by computer modeling. We will delve into pertinent research papers and create our own simulations to challenge the validity of previously accepted methods - continuing to shed new light on our understanding of the universe.

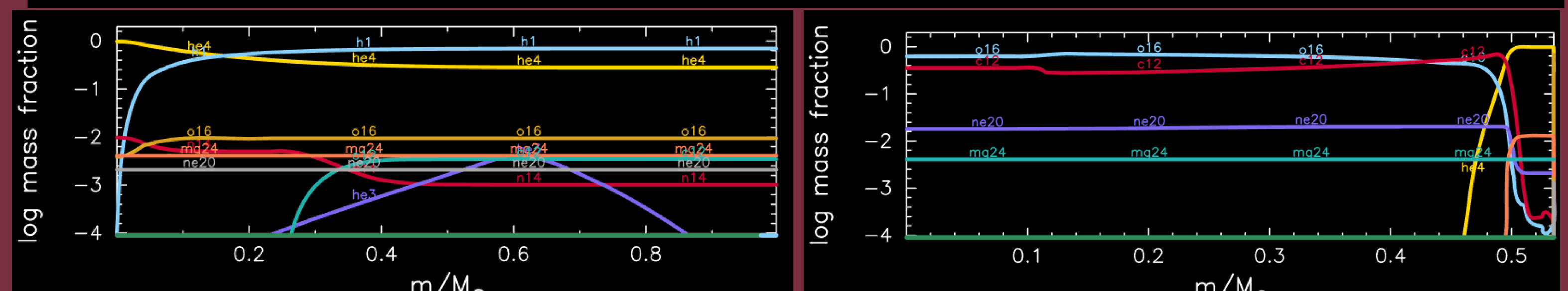

The graphs above contain information about the elemental composition of the modeled star at two different times. When the left data was captured, the star was practically identical in composition and properties to that of our sun. The right model depicts the white dwarf formed near the end of the star's life. The graph on the right shows us that the star evolved into a CO white dwarf.

Methods

The advection-diffusion-reaction (ADR) equation is used to model the behavior and reaction of the nuclear fuel in the star, including the transport of heat, the diffusion of the fuel and ashes, and the reactions that produce energy. In order to solve the ADR equation, astrophysicists must simulate the evolution of the star leading up to the supernova explosion to predict the properties of the explosion itself. This modeling helps improve our understanding of the physics behind SNe Ia and expands our knowledge of the parameters required of the progenitor stars that give rise to them.

Using the Modules for Experiments in Stellar Astrophysics (MESA; Paxton et al. 2011) code's conductive flame model (Schwab, Farmer, & Timmes 2020; hereafter SFT20), we have obtained flame speeds for a broad range of conditions characteristic of massive SN Ia progenitors by solving the energy equation and other pertinent equations through simulations. In this study we use a small 21-isotope nuclear network. The limited size of the nuclear network prevents the creation of a well-defined general equation; however, it does not prevent analysis based on trends. To organize our analysis, the calculated flame speeds have been separated into two different sets of data: a group containing six logarithmically-spaced densities between 1×10^6 and 6×10^6 g cm^{-3} and a second group consisting of densities spanning from 1×10^6 to 1×10^{10} g cm^{-3}.

$$\frac{dE}{dt} + P\frac{\partial(1/\rho)}{\partial t} = \frac{1}{\rho}\frac{\partial}{\partial x}\left(\sigma\frac{\partial T}{\partial x}\right) + \dot{S}$$

The equation on the left is the ADR equation. Solving the coupled nonlinear diffusion equation is necessary to obtain data about behavior of the flame.

Research

Figure 1 presents simulation results from the model of density 1×10^6 g cm^{-3}. The top segment of the left panel in Figure 1 contains information on the composition of the star at different radii. The left side of the graph represents the composition at the center of the star (r=0 cm), and the composition at increasing radii to the right.

Fig.1

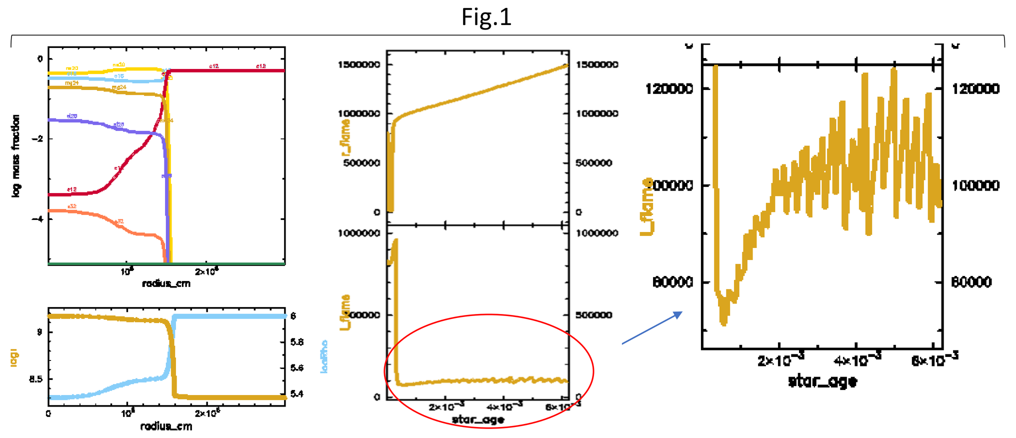

The middle panel in Figure 1 shows the key physical flame properties – flame speed, v_f, and flame thickness, l_f - as a function of time. In Figure 1, the circled section at the bottom of the middle panel is shown enlarged in the right panel, which shows the oscillating behavior of the flame width. Such oscillatory behavior is due to the discrete representation of the flame profile and suggests flame evolution in steady state.

Fig. 2

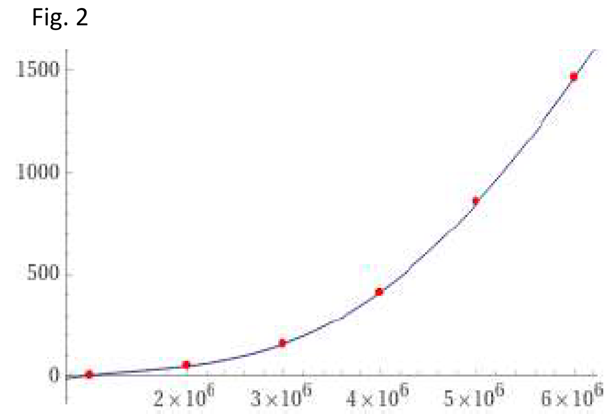

The flame speed for the range of densities between 1×10^6 and 6×10^6 g cm^{-3} is graphed above (Figure 2). The data from the points was used to create a quartic fit (illustrated as the blue line). This equation can reliably be used to estimate flame velocity, v_f for stars with densities within the considered range. This is supported by the residual plot (Figure 3), which shows no systematic trend.

Fig. 3

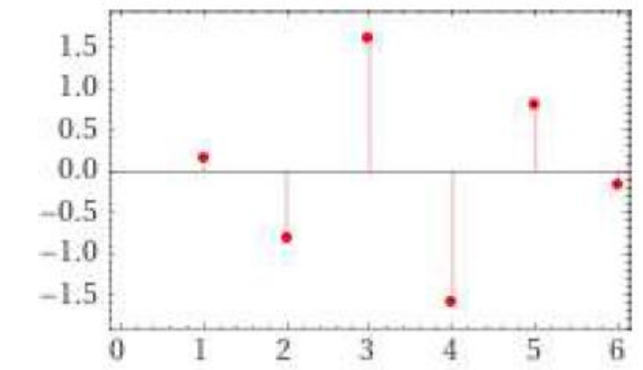

The same approach was taken for the data set spanning a wider range of densities than that of the previous set. Figure 4 contains each data point and the resultant quartic fit. The residual plot for this set of data is shown in Figure 5.

Fig. 4

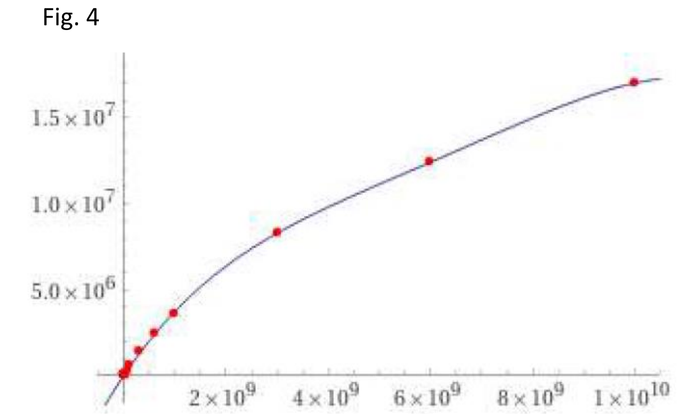

Fig. 5

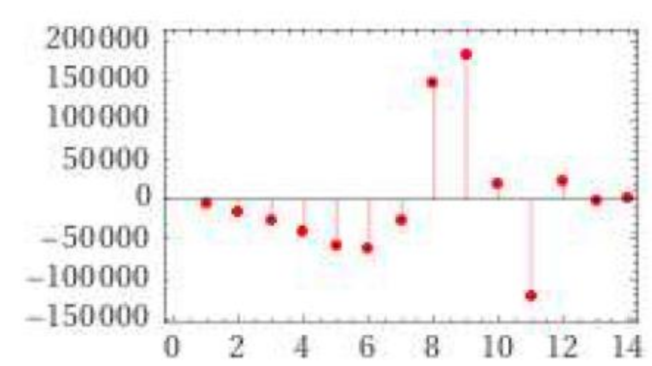

Discussion

As one may have noticed, the regression shown in Figure 5 suggests possible systematic model deviations at low densities, which suggests that there are other external factors that influence the data besides density. Convergence was only possible using specific combinations of initial conditions when modeling. Since we were unable to keep the other variables constant, the trend in regression can be attributed to this variability.

Fig. 6

$$v_{\rm cond} = 92.0\left(\frac{\rho}{2\times10^9}\right)^{0.805}\left[\frac{X(^{12}{\rm C})}{0.5}\right]^{0.889} \ {\rm km\ s^{-1}}$$

In a paper published by Timmes and Woosley in 1992 (TW92), an approximate formula was created to estimate the velocity of the flame speed for densities approximately equal to 9.4×10^9 g cm^{-3} (Figure 6). Looking back to the regression shown in Figure 3, we can notice how we were able to obtain an approximation viable for the smaller range of densities. Without considering Figure 5, the results support the idea of a (mostly) density-and-composition-dependent flame speed, such as Figure 6. However, the data contained in Figure 5 must be acknowledged. Part of this dependency may be attributed to the electron fraction (Y_e).

Arcones et al. (2010; hereafter AMRW10) published a paper examining the behavior of the electron fraction for materials of different densities. It is also stated that the "[w]eak-interaction rates determine the evolution of the electron fraction, which is a key parameter affecting the composition and dynamics of stars in the late stages of stellar evolution and supernovae".

Discussion

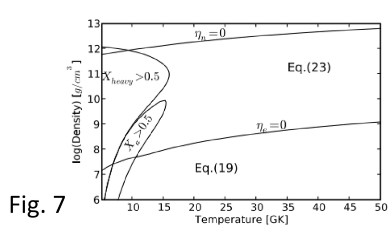

Fig. 7

Figure 7 contains lines which divide the density-temperature graph into sections that can be characterized by the behavior of Y_e. Figure 8 illustrates the minimum Y_e value for density-temperature combinations.

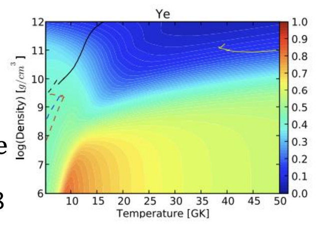

Fig. 8

MESA's conductive flame model begins as an isobaric sphere with no rotation or consideration of the implications that convective mixing or diffusion have on the physics of the star. This simplification is justified by proving convergence of the flame speed for any reasonable set of initial conditions (include formula). Reducing the complexity of the model is adequate for the purpose of estimating the expected flame velocity for modest parameters. When approaching a boundary for the range of convergence, the simplifications of the model inhibit the reliability that the calculated flame speed is representative of the behavior that would be produced by its physical counterpart. A more extensive initial model would be required for these extrema.

As mentioned in the "Methods" section, our simulations were conducted using a network of 21 nuclear isotopes. Previous studies have been conducted (such as SFT20) that show that there is a significant impact that using a smaller nuclear network has on the accuracy of the produced data. SFT20 determined that any network consisting of more than ~200 isotopes was necessary to produce data of adequate accuracy. Since the 21-isotope nuclear network used in our models is much lower than the recommended ~200 isotope minimum, the equations of the quartic fits in Figures 2 and 4 are not accurate (and have therefore not been included). One must also acknowledge potential errors that may arise as a result of data changes by a few orders of magnitude, which would prevent Figures 3 and 5 from telling us accurate information about the fit qualities.

Temperature has been previously observed to have an impact on the flame speed, but this was disregarded in TW92 since the temperature was assumed to be mostly invariant with the tested cases of limited density. Figure 7 and 8 show temperature dependence for the behavior of Y_e. Since Y_e is suggested to have a significant impact on the flame speed, temperature cannot be overlooked when defining a well-defined solution.

The time required to model more complicated simulations must also be considered. The benefits of running a comprehensive set of models to create a new formula that can eliminate the need for future expensive simulations must be compared to the cost of the resources required to run a complete, extensive set of models. To minimize the computation required to produce this complete set of data, we can use a smaller isotope nuclear network for cases that are known to be convergent and dedicate more computational power towards cases with extreme parameters nearing an estimated boundary that may lead to nonconvergent behavior.

Conclusions

Analysis of the data presented in Figure 2 supports TW92's idea of using strictly density to predict the flame speed, however, in the analysis of the data presented in Figure 4, trends in regression appear. Therefore, it is possible to create multiple functions to describe the expected behavior for a small range of densities. However, Figure 5 suggests a need to consider the impact of other parameters on the physical characteristics in order to explain the systematic trend observed at low densities..

To obtain a well-defined equation that accurately predicts the flame velocity for any set of parameters more data must be collected. One should systematically run models for all acceptable combinations of initial conditions. One should then produce a well-defined equation using an optimization algorithm to accurately predict the behavior of any star with acceptable parameters.

Further research should also focus on improving the efficiency of simulations without sacrificing the accuracy of resultant data.

References

- Arcones, A., Martínez-Pinedo, G., Roberts, L. F., & Woosley, S. E. 2010, A&A, 522, A25 (AMRW10)
- Carroll, B and Ostlie, D, Second Edition, An Introduction to Modern Astrophysics (Cambridge University Press)
- Paxton, B., Bildsten, L., Dotter, A., et al. 2011, ApJS, 192, 3 (MESA)
- Schwab, J., Farmer, R., Timmes, F. X., 2020, ApJS, 5,10 (SFT20)
- Timmes, F. X., Woosley, S. E., 1992, ApJS, V.396, p649 (TW92)